Multiple wall dampers for multi-mode vibration control of building structures under earthquake excitation

Mohammad Sabbir Rahman[1a], Seongkyu Chang[*2] and Dookie Kim[1b]

[1]*Department of Civil Engineering, Kunsan National University, Kunsan, Republic of Korea*
[2]*Academic-Industry Cooperation Foundation, Kunsan National University, Kunsan, Republic of Korea*

Abstract.   One of the main concerns of civil engineering researchers is developing or modifying an energy dissipation system that can effectively control structural vibrations, and keep the structural response within tolerable limits during unpredictable events like earthquakes, wind and any kind of thrust load. This article proposes a new type of mass damper system for controlling wideband earthquake vibrations, called Multiple Wall Dampers (MWD). The basic principle of the Tuned Mass Damper (TMD) was used to design the proposed wall damper system. This passive energy dissipation system does not require additional mass for the damping system because the boundary wall mass of the building was used as a damper mass. The multi - mode approach was applied to determine the location and design parameters of the dampers. The dampers were installed based on the maximum amplitude of modes. To optimize the damper parameters, the multi-objective optimization Response Surface Methodology was used, with frequency response and maximum displacement as the objective functions. The obtained structural responses under different earthquake forces demonstrated that the MWD is one of the most capable tools for reducing the responses of multi-storied buildings, and this system can be practically used for new and existing building structures.

Keywords: wall damper; tuned mass damper; vibration control; multi-mode approach; earthquake; multi-storied building

1. Introduction

The construction of civil engineering structures such as high-rise buildings, irregular structures, towers, and long-span bridges is rapidly increasing worldwide, those are very susceptible to excessive vibration loading. Excessive vibration due to external forces like earthquakes and the wind may result in structural damage and undesirable structural performance, and huge loss of life. The catastrophic consequences of recent earthquakes have highlighted the human and economic costs directly related to bridge and building response during an earthquake.

In recent years, considerable attention has been paid to research and efforts to develop a vibration control system for bridges and buildings which can reduce structural response under vibration and keep it within a tolerable limit. One of the promising systems for this application is the tuned mass damper (TMD). To reduce undesirable building vibration, the tuned mass damper works as a passive energy-absorbing device. It is typically comprised of a secondary mass, a spring and a viscous damper attached to the vibration system.   Wang and Lin (2007), Tuscan and

Uluca (2003), Domizio (2015), Nguyen *et a.l* (2012) showed that TMD system is a very effective tool to diminish structural vibration. Luigi and Massimiliano (2008), Bakre and Jangid (2007) found the effective formula to design TMD and relationship between TMD damping ratio and structural damping. Werkle*et al.* (2013) measured the effectiveness of the detuned TMD for a footbridge. Yuxin and Zhitao (2014) demonstrated the advantage of a suspended floor section acting as a massive TMD system for improving seismic performance and structural stability. Multiple tuned mass dampers have also been studied on a large scale to achieve effective response controls for wideband frequencies of earthquakes. Iwanami and Seton (1974), Igusa and Xu (1994), Chen and Wu (2003) showed that more than one TMD effective to control the structural responses under random vibration. Moon (2010) showed that multiple TMDs can be easily and comfortably installed in a smaller space, whereas the installation of a massive single TMD needs a very large space. The effectiveness of multiple tuned mass dampers is depending on the optimal design of damping ratio, frequency, mass ratio and stroke length of MTMD whose has been found from the study of Li and Liu (2002), Mohebbi *et al.* (2015), Chey *et al.* (2015), Lin *et al.* (2010). A comparative study of different control strategies was conducted by Zhang (2014) and concluded that the structural adjacent reaction wall control (STA) system was efficient at lower cost and had other attractive advantages than a mass-semi-active- damper (AMD-2). Chey *et al.* (2010) introduced a new system which combined rubber bearing stiffness with the stiffness of a resettable (semi-

∗Corresponding author, Research Professor
  E-mail: s9752033@gmail.com
[a]Researcher
  E-mail: sabbir.cee@gmail.com
[b]Professor
  E-mail: kim2kie@kunsan.ac.kr

| Uncontrolled model | Controlled model | Mathematical model of controlled structure |
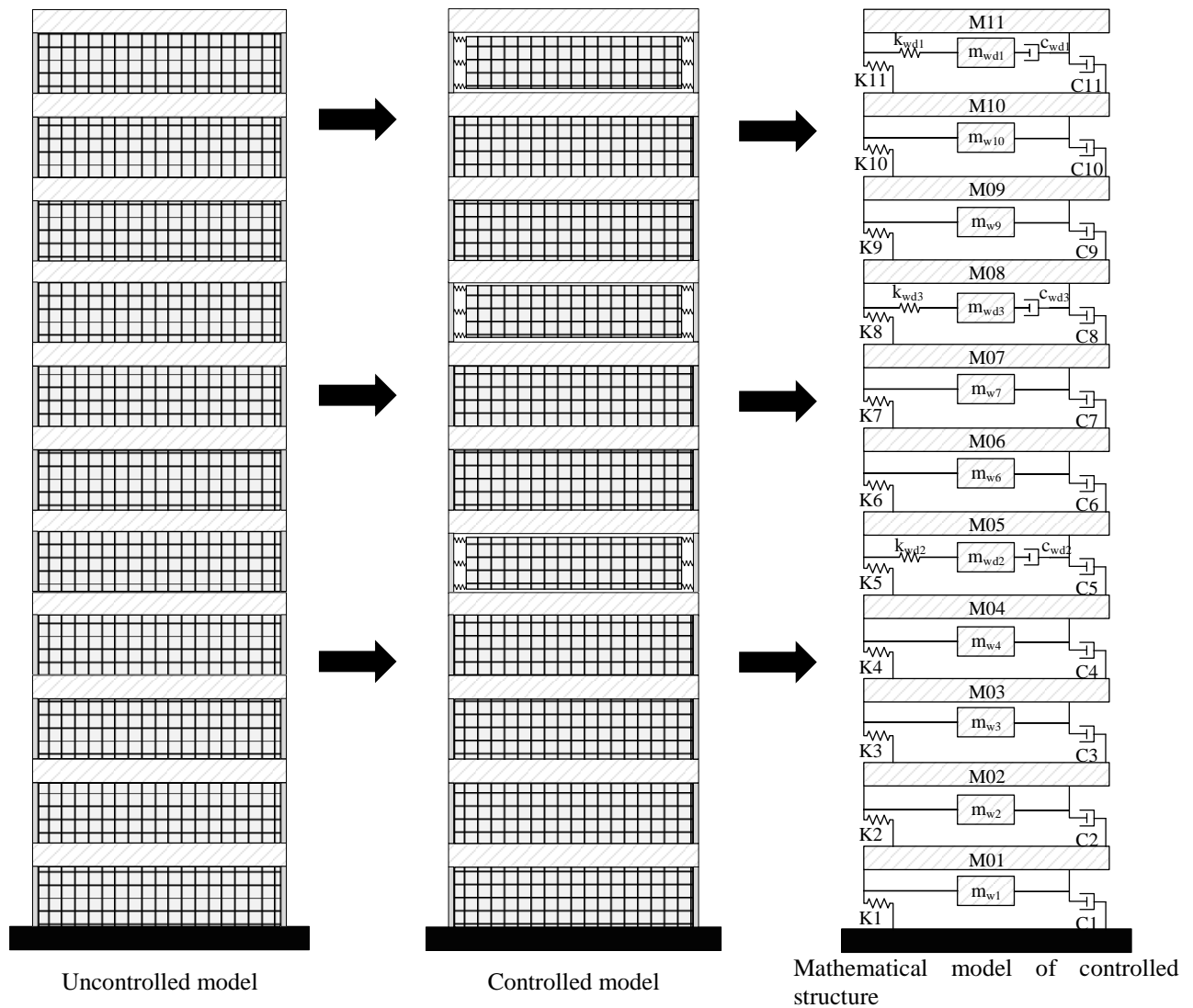
Fig. 1 Structural models with multiple wall dampers (MWD) installed

active) device and works as a semi-active tuned mass damper. Chey *et al.* (2013) proposed an innovative seismic retrofitting strategy, the added stories isolation (ASI) system for multi-degree of freedom (MDOF) system which is able to control broader range ground motions. Xiang and Nishitani (2014) demonstrated the seismic vibration control of building structures using an integrated floor system as a multiple tuned mass damper that is very effective controlling building response under seismic forces.

Multiple tuned mass damper systems, and multiple floor isolation systems have been designed to provide multimode vibration control. To provide control of multiple modes, several modal frequencies of the uncontrolled structure have to be considered in the design of the damper system. Multiple damper systems are very effective at controlling wideband frequency forces such as earthquakes, the wind, or any other random vibration force.

This paper presents a new passive energy dissipation system which utilizes boundary walls as a TMD and combines the advantages of both the boundary wall of the building and the energy dissipation system. The system is called Multiple Wall Dampers (MWD). The main advantage

of this approach is that it does not require additional mass to serve as a damper. The multimode vibration control approach was applied in the design of the wall dampers. Several dampers were installed on different floors of the structure. The damper locations were selected based on the mode shapes of the uncontrolled structure. The damper parameters, frequency ratio, and the damping ratio, were obtained using the multi-objective optimization tool Response Surface Methodology. Importantly, this system is capable of controlling wideband earthquake frequency force excitations. Several earthquake excitations, including El-Centro, Northridge, and California, were applied to evaluate the performance of the proposed MWD. The obtained results showed the MWD provided a satisfactory controlling effect under different band frequency earthquakes.

2. Equation of motion with multiple wall dampers

A representative model of the building structure is shown in Fig. 1, indicating the installation location of the

different Wall Dampers components. The N story building structure was considered to have N-degrees-of-freedom (N-DOF). The walls are connected to the main structural system, with linear stiffness (spring) and linear viscous damping (dashpot) serving as the damper. $M_n(n = 1,2 \ldots N)$ in the figure represents the floor lumped mass of the main structural system, m_w are wall mass of the main system, and $m_{wdj}(j = 1,2 \ldots p)$ represents the TMDs mass. If p is the number of installed wall dampers, and the N-DOF lumped mass structure is excited by a ground acceleration of $\ddot{x}_g(t)$, the equation of motion for the passively controlled system can be described as per Xiang *et al.* (2014),

$$M\ddot{x} + C\dot{x} + Kx = -MH\ddot{x}_g \qquad (1)$$

where $x, \dot{x}$ and $\ddot{x}$ respectively represents the displacement, velocity and acceleration vectors of the system relative to the base point. The dimensions of the matrices can be presented as $(N + p) \times 1$. M, C and K, are the mass, damping and stiffness matrices respectively, where the matrix dimension is $(N + p) \times (N + p)$. H is a unit vector of the $(N + p) \times 1$ matrix dimension.

The global form of M, C and K, are as follows

$$M = \begin{bmatrix} M_{s\,N\times N} & 0_{N\times p} \\ 0_{p\times N} & 0_{p\times p} \end{bmatrix} + \sum_{j=1}^{p} m_{wdj}\, a_j a_j^T \qquad (2)$$

$$C = \begin{bmatrix} C_{s\,N\times N} & 0_{N\times p} \\ 0_{p\times N} & 0_{p\times p} \end{bmatrix} + \sum_{j=1}^{p} c_{wdj}\, b_j b_j^T \qquad (3)$$

$$K = \begin{bmatrix} K_{s\,N\times N} & 0_{N\times p} \\ 0_{p\times N} & 0_{p\times p} \end{bmatrix} + \sum_{j=1}^{p} k_{wdj}\, b_j b_j^T \qquad (4)$$

where, M_s, C_s, and K_s are the mass, damping and stiffness matrices, respectively, of a structure having a matrix

dimension of $N \times N$. In addition, T denotes the transpose of the matrix or vector and m_{wdj}, c_{wdj} and k_{wdj} are the mass, damping and stiffness of the, j-th wall damper, respectively.

M_s can be defined as

$$M_s = M_f + M_w * diag(L) \qquad (5)$$

where, M_f is the mass matrix of the floor, M_w is the mass matrix of the wall and L is the matrix that indicates whether the wall is working as a damper or not. If the wall is working as a damper mass, then the value of this position of the L matrix is 0, and otherwise 1.

The location vectors for the wall dampers are as follows

$$a_j = \begin{bmatrix} 0_{1\times(N+j-1)} & 1 & 0_{1\times(p-j)} \end{bmatrix}^T \ and \qquad (6)$$

$$b_j = \begin{bmatrix} 0_{1\times(loc_j-1)} & -1 & 0_{1\times(N+j-loc_j-1)} & -1 & 0_{1\times(p-j)} \end{bmatrix}^T \qquad (7)$$

The dimension of the location vector is $(N + p) \times 1$, loc_j represents the location of the j-th wall dampers. In Fig. 1, $K_{1\sim11}$ and $C_{1\sim11}$ are structural stiffness and damping. c_{wdj} and k_{wdj} are damper and spring of the wall damper.

Table 1 Details of the structure's materials, with MWD

Item	Value	Unit
Modulus of Elasticity (E)	2.486×10^{10}	Pa
Poisson's Ratio	0.2	-
Density	23563.122	kg/m^3
Shear Modulus (G)	1.036×10^{10}	--
Compressive Strength (*fc'*)	27579032	Pa

(a) Uncontrolled   (b) Controlled by MWD
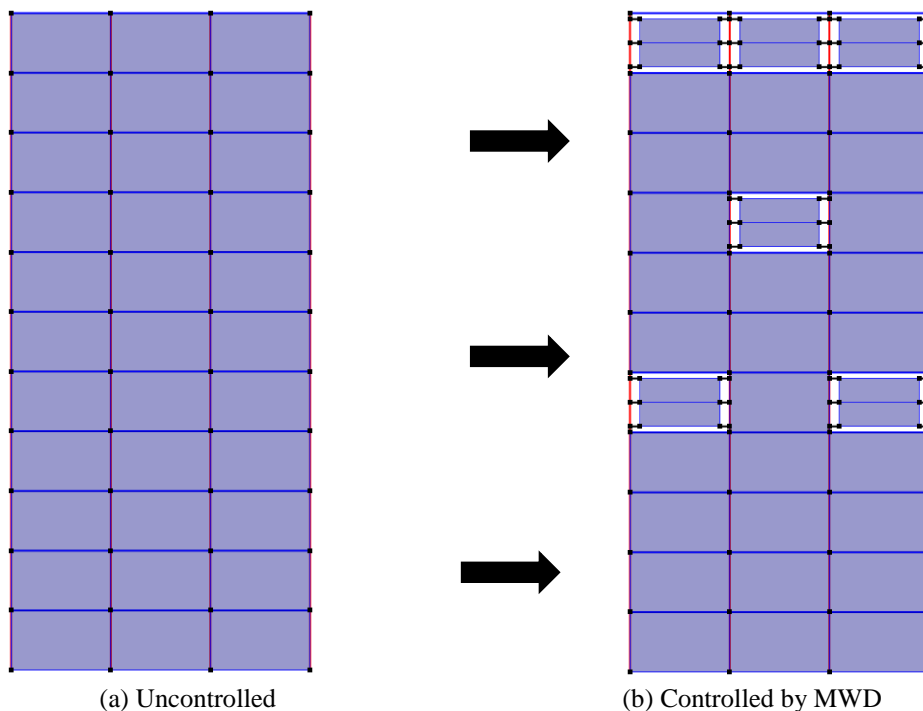
Fig. 2 Structural models in OpenSees with multiple wall dampers

Table 2 Details of the structure's elements, with MWD

Item	Width (mm)	Depth (mm)	Element type
Beam	450	300	Force beam column
Column	500	500	Force beam column
Slab	-	250	Shell
wall	-	150	Shell

Table 3 Time history data of ground motion

	Sweep Acceleration (0 to 10 Hz)	El-Centro Earthquake	North-Ridge Earthquake	California Earthquake
Load steps	6000	2500	2000	2000
Time interval (sec)	0.01	0.02	0.01	0.01
PGA(g)	1.0122	0.348	0.343	0.158

3. Structural model with the multiple wall dampers

In this study, an eleven-story building was considered to analyze the seismic response and 5% structural damping ratio was used in time history analysis because the analysis model is a concrete building. The acceleration of time history was applied as an earthquake load. One directional excitation was performed. The building was modeled in finite element modeling using OpenSees. Three bays of 5 m and 3 m height for each story was considered for this structure. Material properties and element details are provided in Table 1 to Table 2. The building boundary wall does not carry any moment because it is considered to be a brick wall. The Rayleigh damping approach was used to calculate the damping of the uncontrolled structure. Newark's method was used for the time history analysis under different earthquake excitations.

In Fig. 2, the OpenSees building model is represented. Fig. 2(a) presents the uncontrolled eleven story building. Fig. 2(b) illustrates the eleven story building with the adaptive multiple wall damper installed vertically along the story. Dampers were installed on the 5th floor, 8th floor and 11th floor based on the modal parameters of the uncontrolled structure.

4. Application of ground motion

In the present study, four types of ground motion acceleration were applied to evaluate the performance of the multi-mode controlling adaptive multiple wall damper systems in the building structure. One of the types of ground motion is called Sweep acceleration, which contains a frequency of 0 to 10 Hz. In addition, three different types of the earthquake, the El-Centro, California, and North-Ridge were considered. The motive for applying several earthquakes is that different earthquakes contain various distinctive frequencies. As a result, every passive controlling system gives the best performance where the time history signal had to optimize the design of the controlling system. The application of ground motion and

its PGA and time interval are given below in Table 3. Fig. 3 depicts the time history analysis of the applied ground motion.

5. Design of multiple wall dampers

The wall dampers were designed based on the modal parameters. Whole procedure has been shown in Fig. 4. The mode shapes and the effective modal masses were obtained from the modal analysis. More than 90% of the total mass of the building was considered to determine the number of modes that needed to be controlled using the dampers.

From the modal analysis, it was observed that it was necessary to control the first three vibrational modes, because those modes contribute more than 95% of the building mass. Specifically, the first mode contributes 82%, the second mode contributes 9.753% and 3.53% is contributed by the third mode. It was determined that controlling the first vibrational mode required a greater damper mass than the other modes.

The locations of the mode control dampers were selected based on the maximum amplitude of the mode shapes of the structure. Uncontrolled mode shapes are demonstrated in Fig. 5. Considering the mode shapes, the wall dampers were installed on the 11th, 8th floor and 5th floor of the structure. The 11th floor, 8th floor and 5th floor dampers were designed according to the first, third and second modal parameters of the structure. The segment of the wall working as a damper mass on the 11th, 8th and 5th floors is demonstrated in Fig. 2. Three bay walls on the 11th floor work as mass dampers to control the first vibrational mode, two bays wall on the 5th floor and one bay wall on the 8th floor control the second and third modes, respectively. The wall dampers has been designed using RSM method. Using RSM method

The optimum frequency ratio (α_d) and optimum damping ratio (ξ_d) for each damper was obtained using a multi-objective optimization tool called Response Surface Methodology (RSM). Central Composite Design (CCD), which is one type of RSM, was applied to optimize the wall dampers' parameters. The optimum frequency ratio (α_d) and the optimum damping ratio (ξ_d) can be systemically optimized by considering the effect of their interaction on the structural responses. When the structural response under the El-Centro earthquake was optimized, the Frequency Responses (dB) amplitude of each mode and the root mean square of the damper floors displacements $(RMSD)$ were considered as the structural response. The objectives function is defined as

$$J_1 = \max \| dB_{j=1st\ mode},$$
$$\max \| dB_{j=2nd\ mode},$$
$$\max \| dB_{j=p\ mode} \qquad (8)$$

$$J_2 = (RMSD)_{j=p} \qquad (9)$$

where, $\max \| dB_{j\ mode}$ (j=1, 2, …, p) denotes the maximum magnitude of the frequency response function(FRF) for each modal frequency, and $(RMSD)_j$ (j=1, 2, …, p) is the root mean squared displacement of the

(a) Time history and FFT of El-Centro Earthquake

(b) Time history and FFT of California Earthquake

(c) Time history and FFT of North-Ridge Earthquake

(d) Time history and FFT of Sweep Acceleration
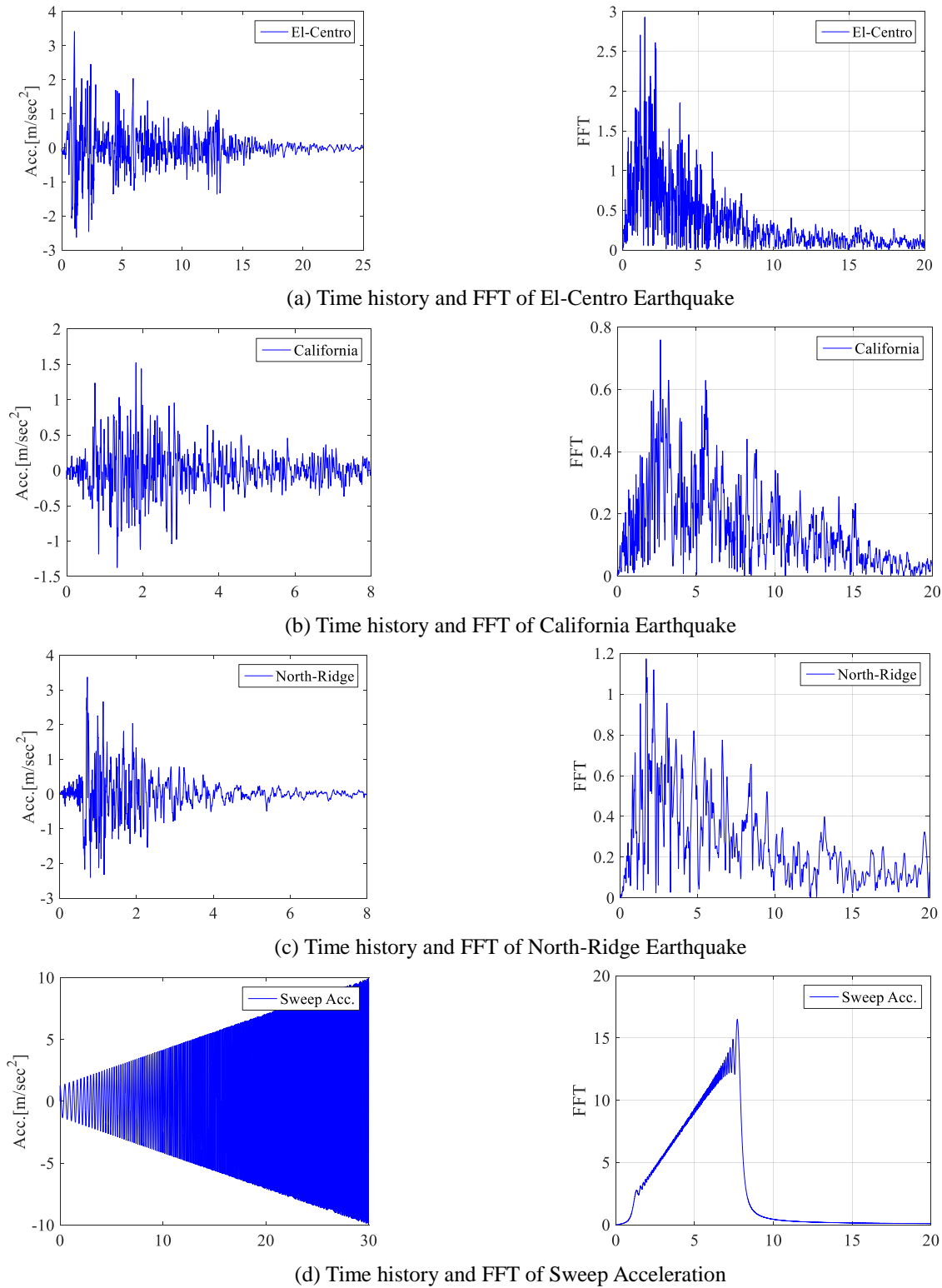
Fig. 3 Applied ground motion

dampers floor.

To perform the Response Surface Methodology (RSM) based optimization, an analysis point is required, which was selected randomly. Using the selected frequencies ratio and damping ratio, the dampers were designed and a structural analysis was performed to determine the structural response. The analysis point and structural responses for each combination are represented in Table 4. In the analysis, point α and ξ are the frequency and damping ratio of the damper, respectively. The structural responses dB_1, dB_2 and dB_3 are the amplitude of the frequency response for the first, second and third modes, and $RMSD_{10F}$, $RMSD_{5F}$ and $RMSD_{8F}$ are the displacement root mean squares of the 11th, 8th and 5th floor, respectively.
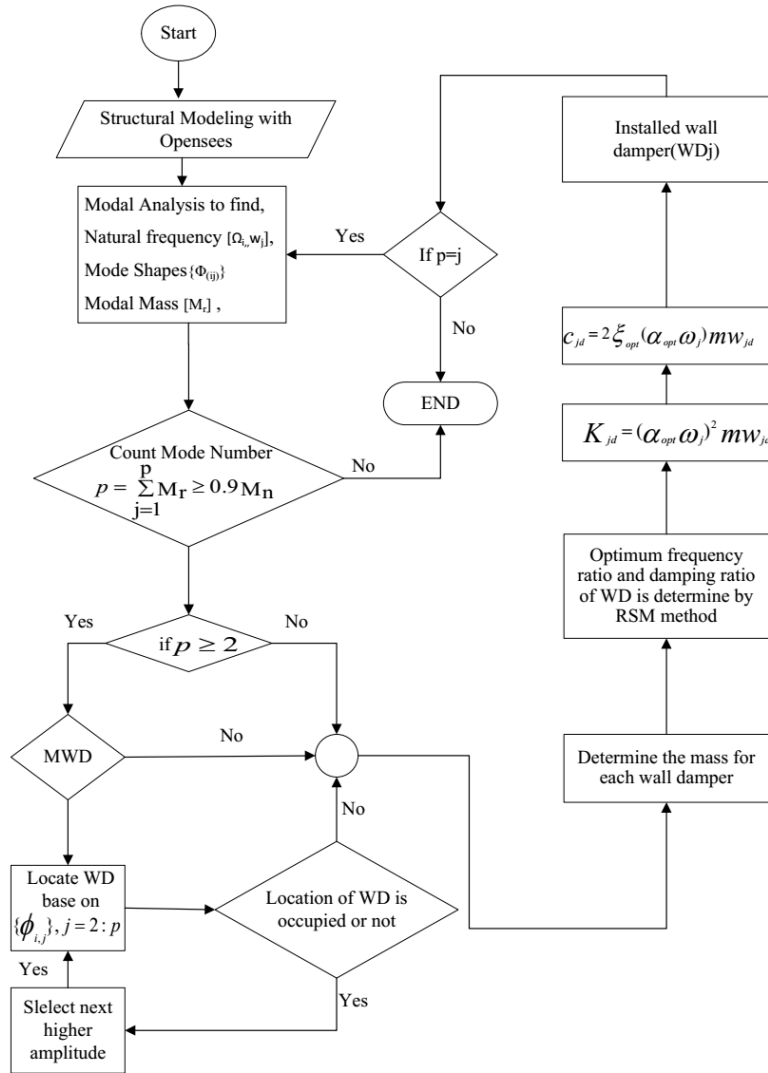
Fig. 4 Design and Installation process of Multiple Wall Dampers (MWD)

Table 4 Analysis point and corresponding structural responses

		Analysis point					Responses		
Run Order	Pt Type	α_d	ξ_d	dB_1	dB_2	dB_3	$RMSD_{10F}$	$RMSD_{5F}$	$RMSD_{8F}$
1	0	0.925	0.125	5.311	2.760	1.789	0.022	0.010	0.020
2	1	0.850	0.200	6.553	3.178	2.030	0.025	0.010	0.022
3	1	0.850	0.050	9.347	3.802	2.206	0.030	0.010	0.026
4	-1	0.819	0.125	8.595	3.644	2.170	0.029	0.010	0.026
5	1	1.000	0.200	4.040	1.847	1.324	0.019	0.010	0.016
6	-1	0.925	0.231	3.974	2.278	1.613	0.019	0.010	0.017
7	1	1.000	0.050	6.471	2.595	1.680	0.025	0.010	0.021
8	-1	1.031	0.125	5.983	2.156	1.589	0.023	0.010	0.019
9	-1	0.925	0.019	8.236	3.600	2.050	0.027	0.010	0.024

A design matrix involving the quadratic terms was employed to develop the equations to estimate the structural performance with the MWD. Based on multiple linear regressions, the variable coefficients were derived following Lee *et al.* (2015)

$$\hat{y} = D.b \qquad (10)$$

where, $\hat{y}$ is the predicted response, which is stated as the product of the design matrix, D, and the corresponding coefficients, b. The vector of the corresponding coefficients
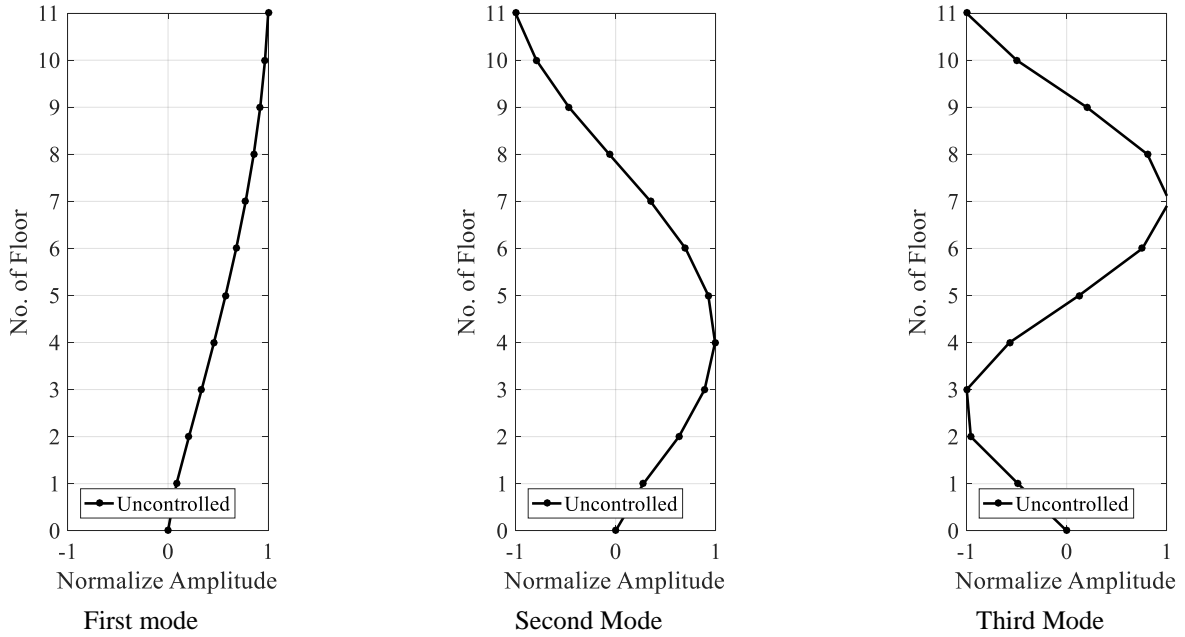
Fig. 5 First three mode shapes of the uncontrolled structure

Table 5 Quadratic models for frequency amplitude (dB) and RMS of displacement (m)

	Items	Model Equation	R^2
WD_1	dB_1	$171 - 334.7(\alpha_1) - 50.3(\xi_1) + 171.6(\alpha_1{}^2) + 66.4(\xi_1{}^2) + 16.1(\alpha_1\xi_1)$	98.46%
	$RMSD_{11F}$	$0.3783 - 0.724(\alpha_1) - 0.0609(\xi_1) + 0.3743(\alpha_1{}^2) + 0.0885(\xi_1{}^2) + 0.0001(\alpha_1\xi_1)$	99.26%
WD_2	dB_2	$18.4 - 28.4(\alpha_1) - 3.6(\xi_1) + 9.6(\alpha_1{}^2) + 13.1(\xi_1{}^2) - 5.5(\alpha_1\xi_1)$	99.47%
	$RMSD_{5F}$	$0.0112 - 0.0018(\alpha_1) - 0.0009(\xi_1) + 0.00085(\alpha_1{}^2) + 0.0006(\xi_1{}^2) + 0.00075(\alpha_1\xi_1)$	98.51%
WD_3	dB_3	$9.45 - 13.6(\alpha_1) - 5.04(\xi_1) + 6.02(\alpha_1{}^2) + 1.76(\xi_1{}^2) - 8.00(\alpha_1\xi_1)$	96.43%
	$RMSD_{8F}$	$0.2709 - 0.5028(\alpha_1) - 0.0231(\xi_1) + 0.2559(\alpha_1{}^2) + 0.0652(\xi_1{}^2) - 0.0283(\alpha_1\xi_1)$	99.25%

*WD_1, WD_2 and WD_3: Wall damper for 1st, 2nd and 3rd vibration mode control

is the pseudo inverse of D and the experimental response

$$b = (D'.D)^{-1}.D'.y \quad (11)$$

The coefficients indicate the behavior of different factors on the response where various models can be described. The quadratic models were derived for this study based on CCD, and the coefficient magnitude indicates the contribution of various factors to the responses. The quadratic models (Rajmohan *et al.* 2013) as expressed below

$$\hat{y} = b_0 + \sum_{i=1}^{k} b_i X_i + \sum_{i=1}^{k} b_{ii} X_i{}^2 + \sum_{i=1}^{k} b_{ij} X_i X_j + \varepsilon (12)$$

from the derived model demonstrated that the frequency ratio of the damper has a greater influence on improving the structural response under seismic excitation. It was found that the value of R^2 is high, which means the model can be considered adequate. The quadratic models, R^2 for frequency responses (FR) and the root mean square of displacements (RMSD) for each damper are shown in Table 5.

Fig. 6 demonstrates the three-dimensional response surface plot of the dynamic structural responses (RMS displacement and frequency amplitude) verses two parameters (damping ratio and frequency ratio) of wall dampers. This figure shows the displacement root mean square of the 11th, 5th and 8th floor, and the frequency amplitude of the first, second and third modes because WD_1, WD_2, and WD_3 are designed to control the first, second and third modal vibrations under the El-Centro earthquake. It is clear from the response surface plot that frequency ratio is a more important factor than the damping ratio for designing the MWDs. The lowest point of these surface is optimum damping ratio and frequency ratio for each wall damper. In Table 7 optimum combination of frequency ratio and damping ratio has been provided those combination the wall dampers are performed better.

The multiple performance optimizations of the wall dampers parameters were carried out using the response surface methodology, based on the desirability function approach. The optimization analysis was carried out using the Design-Expert package (Minitab software). The goal set, lower limits, upper limits, weights, and the importance of the factors given are presented in Table 6.

The desirability-based approach provides the best solution. The best solutions obtained for the optimization are presented in Table 7. The optimization was carried out for a combination of goals, and those goals were applied to the factors and responses. The goal used for the responses was "minimize" and the goal used for the factors as "within range". A weight can be assigned to a goal to

(a) 3D graph showing the interaction effect on RMS_{11} and dB_1e for WD_1

(b) 3D graph showing the interaction effect on RMS_5 and dB_2 for WD_2

(c) 3D graph showing the interaction effect on RMS_8 and dB_3 for WD_3
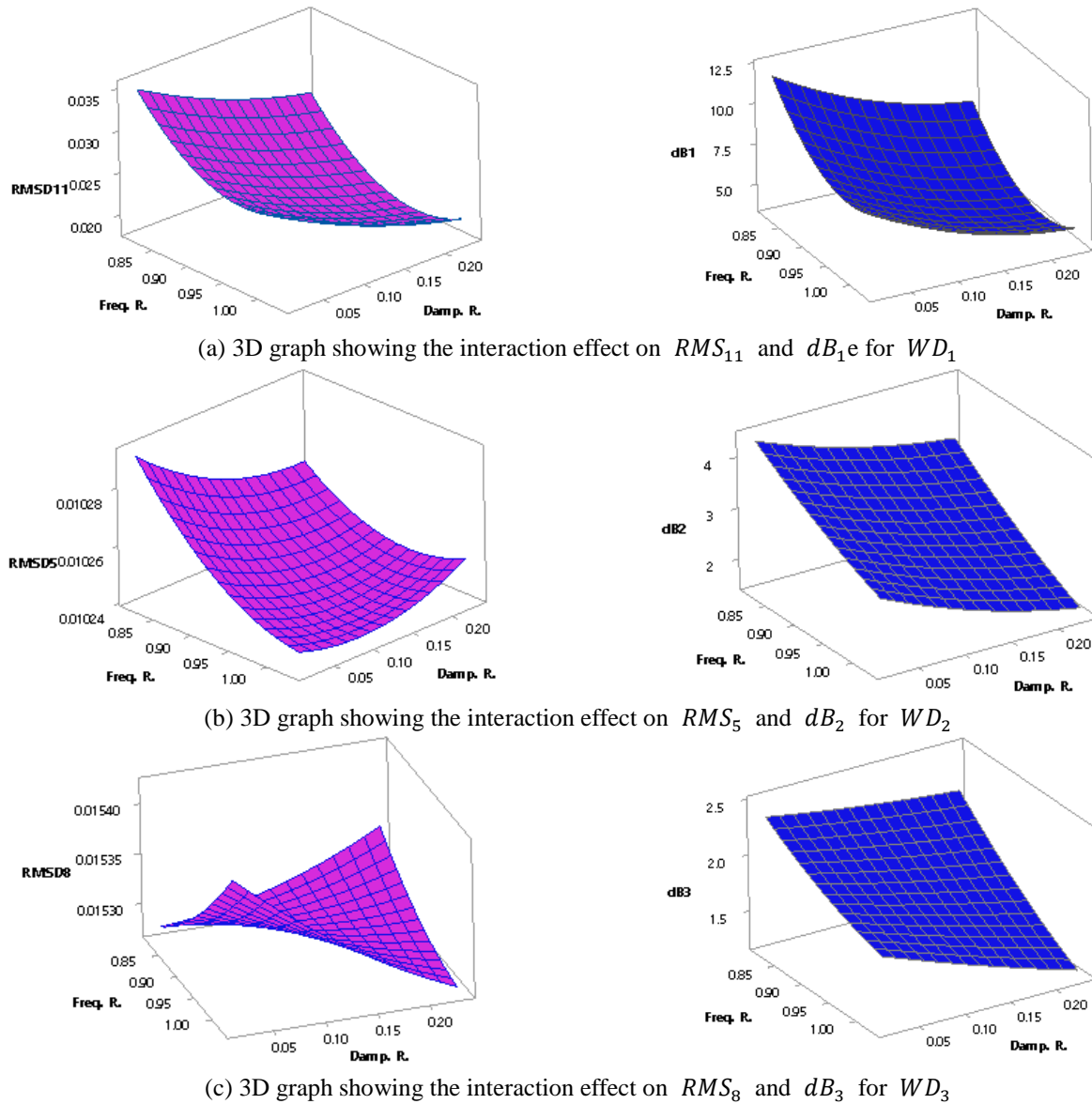
Fig. 6 Three-dimensional response surface plots of the dynamic structural responses verses frequency ratio and damping ratio

Table 6 Goal for optimization wall damper parameters

	Items	Goal	Lower	Target	upper	Weight	Importance
WD_1	dB_1	Minimize	3.974	3.974	9.347	1	1
	$RMSD_{11F}$	Minimize	0.018	0.018	0.030	1	1
WD_2	dB_2	Minimize	1.84	1.84	3.8	1	1
	$RMSD_{5F}$	Minimize	0.010	0.010	0.011	1	1
WD_3	dB_3	Minimize	1.324	1.324	2.63	1	1
	$RMSD_{8F}$	Minimize	0.016	0.016	0.026	1	1

Table 7 Best global solution for obtaining the TMDs parameters

Items	Frequency Ratio(α)	Damping Ratio(ξ)	Displacement RMS		FR Amplitude	
			Predicted	From Analysis	Predicted	From Analysis
WD_1	0.977	0.231	0.0184	0.0179	3.80	3.52
WD_2	0.986	0.207	0.010	0.011	1.88	2.26
WD_3	0.926	0.162	0.0152	0.0172	1.322	1.42

adjust the shape of its particular desirability function. From the desirability analysis, the individual and composite desirability was as close to 1 as possible.

From the analysis of the results, the optimal solutions obtained for the three types of WDs were 0.9464, 1.03 and 1.03 frequency ratio for WD_1, WD_2 and WD_3 respectively, whereas the damping ratios for each of the MWDs were 0.231, 0.16 and 0.231. The predicted

frequency response amplitudes for the first, second and third modes were 3.80, 1.88 and 1.322dB respectively, whereas from the analysis the obtained responses were 2.926, 1.313 and 1.757dB. The displacement root mean square of the 11th, 5th and 8th were 0.0179, 0.010 and 0.0152 as obtained from the structural analysis, though the predicted responses were 0.0184, 0.010 and 0.0152, as represented in Table 7.

First mode   Second Mode   Third Mode
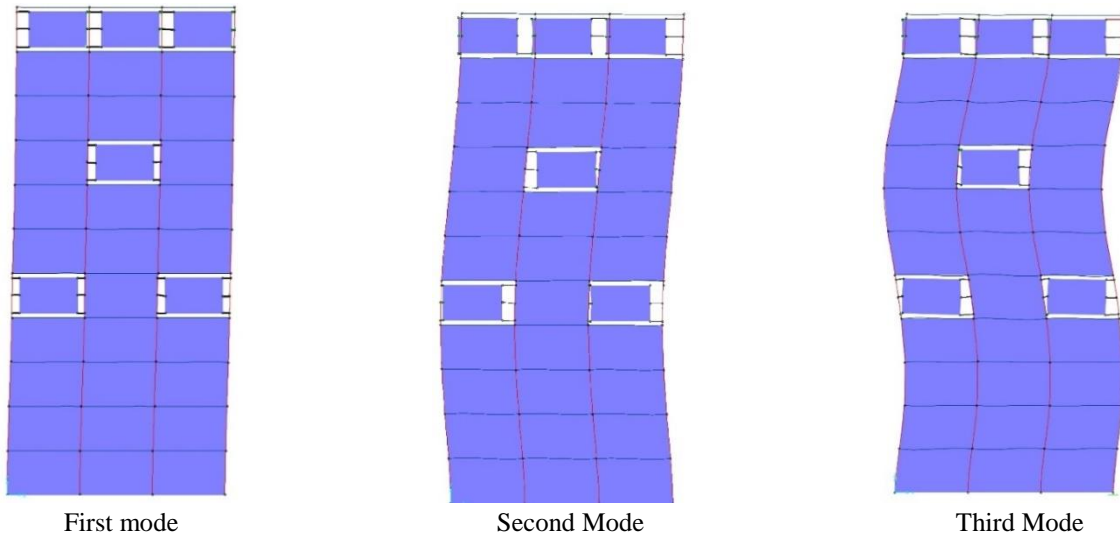
Fig. 7 First three mode shapes for the structure with the Wall Dampers
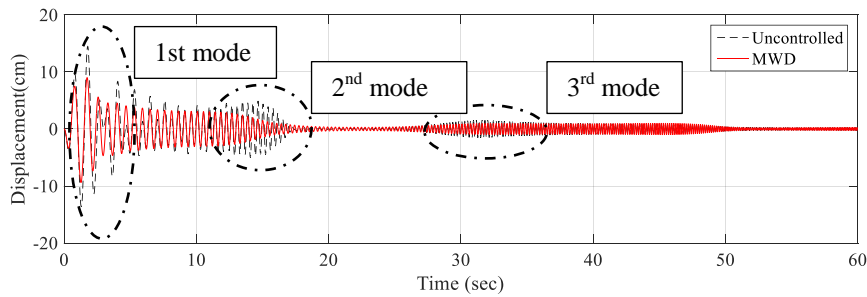
(a) Top floor displacement of the uncontrolled structure, and the structure with three modes controlled
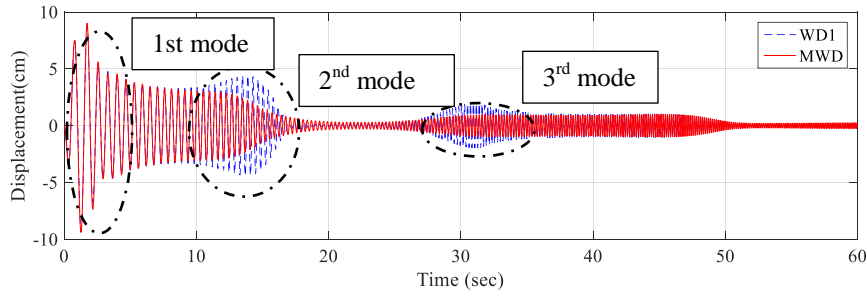
(b) Top floor displacement of one mode, and the structure with three modes controlled
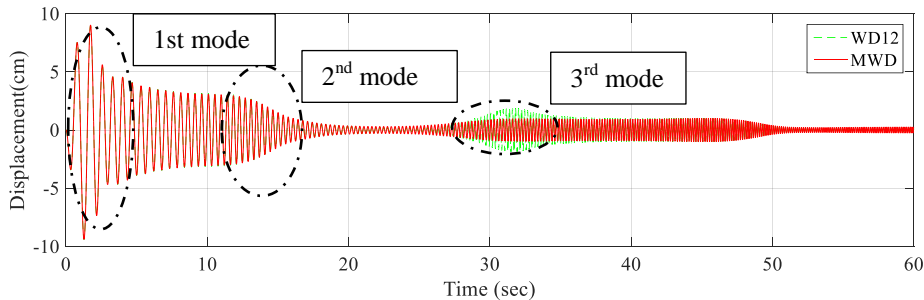
(c) Top floor displacement of two modes and the structure with three modes controlled

Fig. 8 Top floor displacement of the uncontrolled structure, and the structure with different modes controlled, under sweep acceleration

The stiffness and damping of the dampers were obtained from $k_{dj} = m_{wdj}(\alpha_d \omega_j)^2$ and $C_{jd} = 2(\alpha_d \omega_j)\xi_d m_{wdj}$,where j indicates the dampers' numbers. The Wall damper parameters are provided in Table 8.

6. Results and discussion of MWD system

To establish the effectiveness of the MWD, the different types of responses were compared. The comparisons of the

Table 8 Wall dampers properties

Item	WD_1	WD_2	WD_3
Mass (Kg)	3458.81	3458.81	3458.81
Stiffness(N/m)	15387.47	156996.39	485662.09
Damping(N-Sec/m)	1376.58	2928.20	7733.65

Table 9 Natural frequencies of the uncontrolled and controlled structures

Mode No.	Uncontrolled(Hz)	MWD(Hz)
First Mode	0.852	0.89
Second Mode	2.59	2.73
Third Mode	4.45	4.72

uncontrolled and controlled responses for the modal parameters of the structure, displacement, base shear force, and frequency response, are shown in Fig. 8 to Fig. 11. From these figures it is clear that the MWD is capable of controlling several vibrational modes under wideband earthquake excitation.

A modal analysis was carried out after the design and installation of the adaptive wall mass damper, to determine the effect of the wall dampers with respect to the modal parameters. Table 9 indicates the natural frequency for different cases. And Fig. 7 shows the mode shapes for the proposed system with wall dampers.

Fig. 8 shows the displacement response of the structure under sweep acceleration. Sweep acceleration has wideband frequency and a frequency range of 0 to 10 Hz. From the resulting displacement, it can be clearly observed that the vibrational mode controls the effect of the MWD. The sweep acceleration was applied with different control systems, including a control system for one, two and three vibrational modes. As the figure shows, several peak displacements occur under sweep acceleration. Several peaks indicate the resonance effect for several natural frequencies of the structure. From the displacement response, it was observed that there were four resonance effects, for the first, second, third and fourth resonances, occurring at 0 to 8 sec, 10-18 sec, 28-38 sec and 42-50 sec, respectively. The first, second, third and fourth resonances which occurred due to the force frequency were matched with the first, second and fourth modal frequencies of the structure. So, the MWD is capable of suppressing the first three resonance effects, and one (WD1), two (WD12) and three wall dampers (MWD) were able to control first one, first two and first three modes respectively.

Fig. 9 shows the top floor displacement for the uncontrolled structure and the structure controlled by the MWD when subjected to the El-Centro, California, and North-Ridge ground motions. From the obtained results, it was observed that the uncontrolled maximum displacement of the structure was 15.18 cm, 2.13 cm and 5.37 cm, whereas the controlled displacement with MWD was 8.64 cm, 1.65 cm, and 3.45 cm for the El-Centro, California and North-Ridge earthquakes, respectively. The rate of reduction of the maximum top floor displacements of the uncontrolled structure were 44.30%, 22.74% and 34.53 % under for the El-Centro, California, and North-Ridge
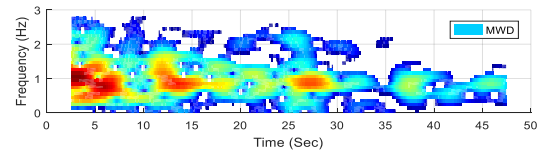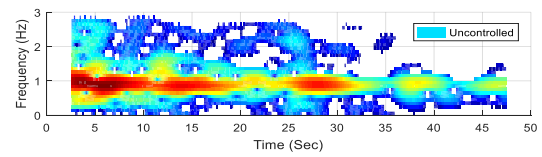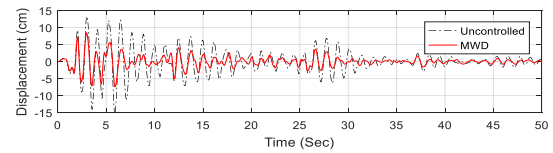
(a) El-Centro Earthquake
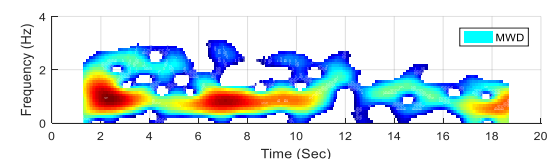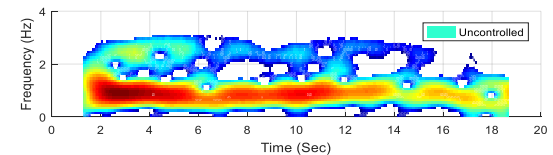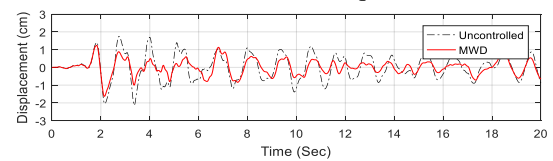
(b) California Earthquake
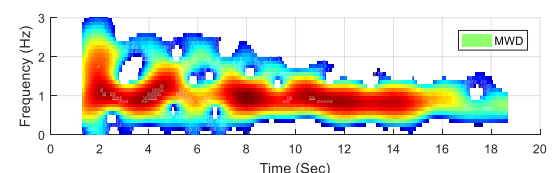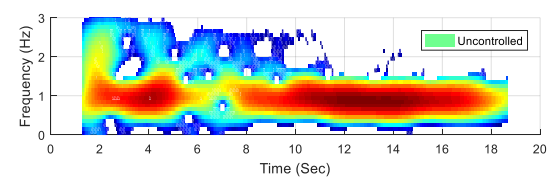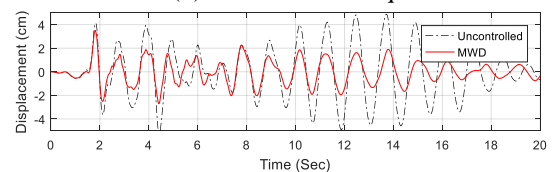
(c) North-ridge Earthquake

Fig. 9 Top floor displacement and time-frequency analysis results under Earthquakes

earthquakes, respectively. The wall damper's stroke length for $WD1$ was 181.15 mm, 25.19 mm and 54.39 mm for the El-Centro, California, and North-Ridge earthquakes, respectively. MWD is also passive type controller and TMD generally tuned in phase about 90degrees of the structural

(a) Base shear forces under the El-Centro Earthquake

(b) Base shear forces under the California Earthquake

(c) Base shear forces under the North-Ridge Earthquake
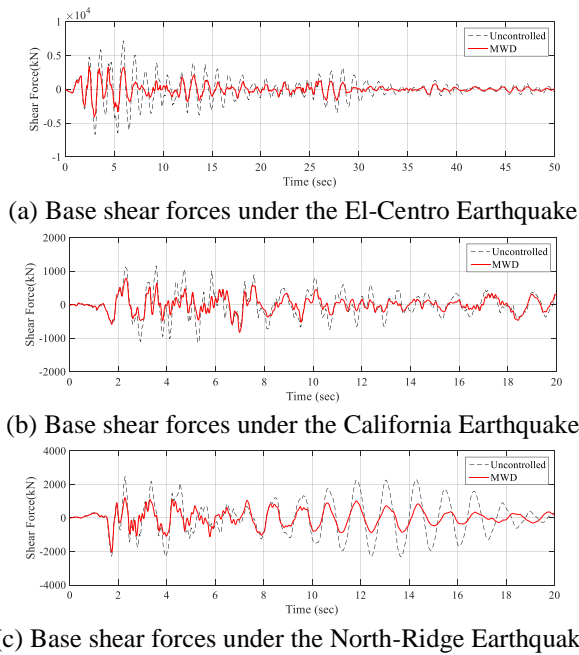
Fig. 10 Base shear force comparison of the uncontrolled structure and the controlled structure by MWD under different Earthquakes

(a) FRF curve under the El-Centro earthquake

(b) FRF curve under the California earthquake

(c) FRF curve under the North-Ridge earthquake

(d) FRF curve under the Sweep acceleration

Fig. 11 Frequency response curves under different excitations

response. So the responses by a first shock acting on the building can not be significantly reduced by MWD. In Fig. 9(c), it shows that the decreases of the responses in first peak are marginal rather than post peaks. Fig. 9 also shows the results of the time-frequency analysis results which were drawn from each displacement data using a spectrogram function in Matlab. Fig. 9(a) shows strongly the frequency components in around a 1Hz in uncontrolled while those areas are reduced in the controlled results. Fig. 9(b) and Fig. 9(c) also show the frequency area over time under for the California and North-Ridge earthquakes, respectively. The red color area shows a tendency reducing when the MWDs were installed in the structure.

Fig. 10 shows the time history response of the base shear for the uncontrolled structure and the structure controlled by MWD for different earthquake excitations. From the time history response of each curve of the earthquake, it is clear that the MWD is capable of reducing the base shear force effect of the structure under a broad range of earthquake excitations. The percent reduction in the maximum base shear force was 42.86%, 28.64% and 16.62% for the El-Centro, California, and North-Ridge earthquakes, respectively.

Fig. 11 shows the results of the acceleration frequency response curve for the uncontrolled structure and the structure controlled by the MWD under the El-Centro, California and North-Ridge Earthquakes, and under sweep acceleration (where the frequency varies from 0 to 10 Hz). The maximum frequency response amplitudes of the uncontrolled structure were 12.61 dB, 11.06 dB, 12.11dB and 13.29 dB, and for the controlled structure with the MWD, they were 3.52 dB, 7.15 dB, 3.48 dB and 3.678 dB, for the first mode under the El-Centro, California, North-Ridge Earthquakes, and the Sweep acceleration,
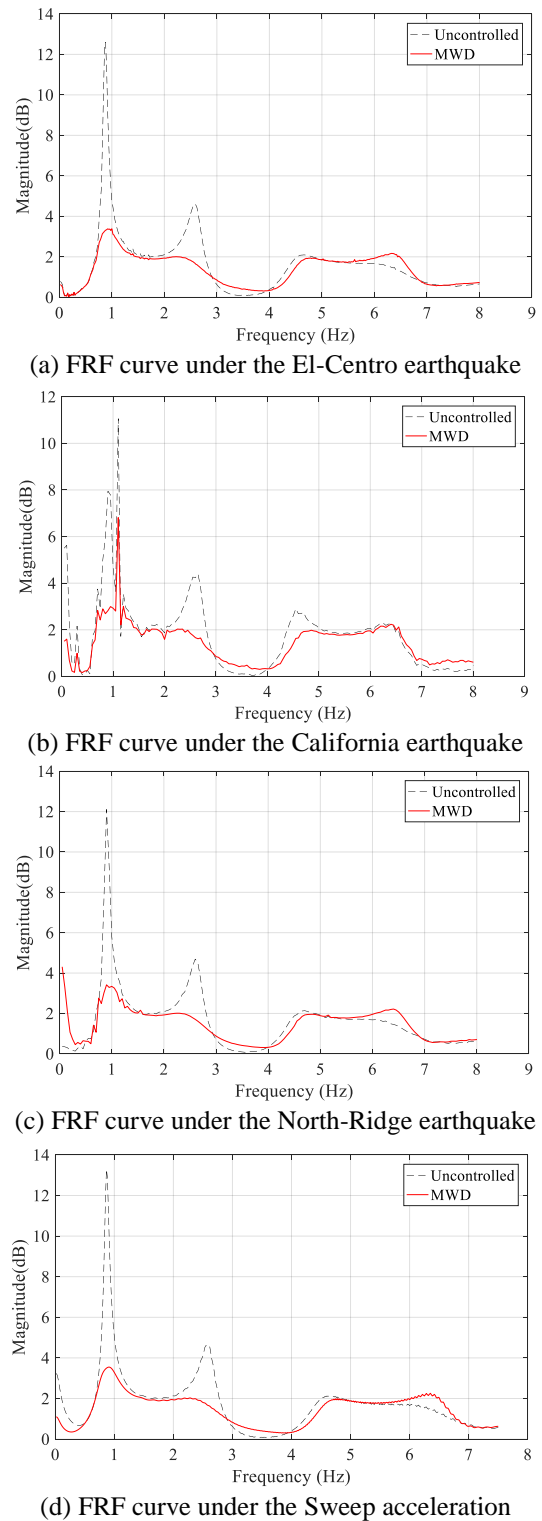
respectively. For the second mode the maximum frequency response amplitudes were 4.62 dB, 4.39 dB, 4.7 dB and 4.63 dB for the uncontrolled structure, and 2.26 dB, 2.286 dB, 2.274 dB and 2.29 dB for the structure controlled with the MWD under the El-Centro, California, North-Ridge Earthquakes, and the Sweep acceleration, respectively. For the third mode, they were 2.1 dB, 2.90 dB, 2.11 dB and

2.13 dB for the uncontrolled structure, and 1.418 dB, 1.42 dB, 1.44 dB and 1.488 dB for the structure controlled by the MWD.

From the performance demonstrated by the MWD, it is clear that the MWD is capable of controlling several modal frequencies of the uncontrolled structure.

7. Conclusions

This work proposed a new vibration control system, which was installed on different floors of a building structure and was able to control several modal vibrations under random vibration conditions. This system can serve as a damper as well as a boundary wall in the building structure. This new damper system is called the Multiple Wall Damper (MWD). The locations of the dampers were selected based on the maximum mode shape amplitude. The multi-objective optimization tool Response Surface Methodology (RSM) was used to determine the optimal frequency ratio and the damping ratio of the dampers. The modeling of the structure and the simulation were carried out using OpenSees.

To evaluate the performance of the MWD, the test results of the structure controlled with the MWD were compared with those obtained for an uncontrolled version of the same structure.

The following conclusions can be drawn from the trend of the results of this study.

• The MWD was significantly more efficient and practical in reducing the response of the building, and did not require any additional mass for the dampers because the mass of the boundary wall of the building structure was used as the mass of the damper system. Although MWD is a passive type mass damper, the results showed a remarkable reduction in the maximum top displacement after first shock.

• The dominant mode shapes amplitude of the building was primarily considered to select the locations of the dampers. The design and installation of the Wall Dampers focused on the modal parameters of the first three modes because they contributed about 95% of the structural mass.

• The rate of response reduction in the uncontrolled top displacement was 44.30%, 22.74% and 34.53 % for the El-Centro, California and North-Ridge earthquakes, respectively.

• The amplitude of the frequency response reduction for first mode frequency was about 71.93%, 35.35%, 71.23% and 72.32% under the El-Centro, California, Northridge earthquakes, and the sweep acceleration, respectively. For the second mode frequency, it was about 51.03%, 47.97%, 51.55% and 50.62%. Moreover, for the third mode, it was 32.39%, 51.11%, 32.39 % and 29.81%.

• These results clearly indicate that the MWD is capable of controlling wideband frequency earthquake forces.

In order prevent the collapse of the building and increase the effect of the MWD, it is need to study about using the MWD and other dampers simultaneously for further research.

References

Bakre, S.V. and Jangid, R.S. (2007), "Optimum parameters of tuned mass damper for damped main system", *Struct. Control Hlth. Monit.*, **14**(3), 448-470.

Chen, G. and Wu, J. (2003), "Experimental study on multiple tuned mass dampers to reduce seismic responses of a three-storey building structure", *Earthq. Eng. Struct. Dyn.*, **32**(5),793-810.

Chey, M., Chase, J.G., Mander, J.B. and Carr, A.J. (2015), "Aseismic smart building isolation systems under multi-level earthquake excitations: Part II, energy-dissipation and damage reduction", *Front. Struct. Civil Eng.*, **9**(3), 297-306.

Chey, M., Geoffrey, C.J., Mander, J.B. and Carr, A.J. (2010), "Semi-active tuned mass damper building systems: Application", *Earthq. Eng. Struct. Dyn.*, **39**(1),69-89.

Chey, M., Geoffrey, C.J., Mander, J.B. and Carr, A.J. (2013), "Innovative seismic retrofitting strategy of added stories isolation system", *Front. Arch. Civil Eng. China*, **7**(1), 13-23.

Domizio, M., Ambrosini, D. and Curadelli, O. (2015), "Performance of TMDs on nonlinear structures subjected to near-fault earthquakes", *Smart Struct. Syst.*, **16**(4), 725-742.

Igusa, T. and Xu, K. (1994), "Vibration control using multiple tuned mass dampers", *J. Sound Vib.*, **175**(4), 491-503.

Izanami, K. and Seton, K. (1984), "Optimum design of dual tuned mass dampers and their effectiveness", *Japan Soc. Mech. Eng.*, **50**(1), 44-52.

Lee, T.Z.E., Krongchai, C., Lu, N.A.L.M.I., Kittiwachana, S. and Sim, S.F. (2015), "Application of central composite design for optimization of the removal of humic substances using coconut copra", *Int. J. Indus. Chem.*, **6**(3), 185-191.

Li, C. and Liu, Y. (2002), "Further Characteristics for Multiple Tuned Mass Dampers", J. Struct. Eng., 128(10), 1362-1365.

Lin, C.C., Wang, J.F., Lien, C.H., Chiang, H.W. and Lin, C.S. (2010), "Optimum design and experimental study of multiple tuned mass dampers with limited stroke", *Earthq. Eng. Struct. Dyn.*, **39**(14), 1631-1651.

Luigi, P. and Massimiliano, D.I. (2008), "Robust design of a single tuned mass damper for controlling torsional response of asymmetric-plan systems", *J. Earthq. Eng.*, **13**(1), 108-128.

Mohebbi, M., Rasouli, H. and Moradpour, S. (2015), "Assessment of the design criteria effect on performance of multiple tuned mass dampers", *Adv. Struct. Eng.*, **18**(8), 1141.

Moon, K.S. (2010), "Vertically distributed multiple tuned mass dampers in tall buildings: performance analysis and preliminary design", *Struct. Des. Tall Spec. Build.*, 19(3), 347-366.

Nguyen, T., Saidi, I., Gad, E., Wilson, J. and Haritos, N. (2012), "Performance of distributed multiple viscoelastic tuned mass dampers for floor vibration applications", *Adv. Struct. Eng.*, **15**(3), 547-562.

Rajmohan, T. and Palanikumar, K. (2013), "Application of the central composite design in optimization of machining parameters in drilling hybrid metal matrix composites", *Measur.*, **46**(4), 1470-1481.

Tuscan, S.S. and Uluca, O. (2003), "Reduction of earthquake response of plane frame buildings by viscoelastic damper", *Eng. Struct.*, 25(14), 1755-1761.

Wang, A.P. and Lin, Y.H. (2007), "Vibration control of a tall building subjected to earthquake excitation)", *J. Sound Vib.*,

299(4-5), 757-773.

Werkle, H., Butz, C. and Tatar, R. (2013), "Effectiveness of "Detuned" TMD's for beam-kike footbridges", *Adv. Struct. Eng.*, **16**(1), 21-31.

Xiang, P. and Nishitani, A. (2014), "Seismic vibration control of building structures with multiple tuned mass damper floors integrated", *Earthq. Eng. Struct. Dyn.*, **43**(6), 909-925.

Yuxin, L. and Zhitao, L. (2014), "Seismic performance and storey-based stability of suspended buildings", *Adv. Struct. Eng.*, **17**(10), 1531.

Zhang, C. (2014), "Control force characteristics of different control strategies for the wind-excited 76-story benchmark building structure", *Adv. Struct. Eng.*, **17**(4), 543-560.

CC